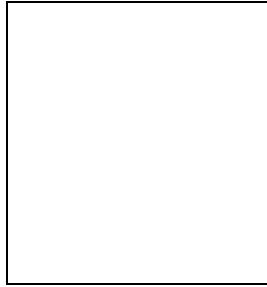


CONSTRAINING THE COSMOLOGICAL PARAMETERS FROM GRAVITATIONAL LENSES WITH SEVERAL FAMILIES OF IMAGES

G. GOLSE, J.-P. KNEIB and G. SOUCAIL

*Laboratoire d'Astrophysique, UMR 5572, Observatoire Midi-Pyrénées
14 avenue E.-Belin, F-31400 Toulouse, France*



The knowledge of the redshift of multiple images in cluster-lenses allows to determine precisely the total projected mass within the Einstein radius. The observation of various multiple images in a same cluster is opening new possibilities to constrain the curvature of the universe. Indeed, although the influence of Ω_m and Ω_λ on the images formation is of the second order, observations of many multiple images at different redshifts formed by a regular cluster-lens should allow to constrain very accurately the mass distribution of the cluster and to start to be sensitive to the cosmological parameters entering the diameter angular distances. We present, analytical expressions and numerical simulations that allow us to compute the expected error bars on the cosmological parameters provided an HST/WFPC2 resolution image and spectroscopic redshifts for the multiple images. Numerical tests on simulated data confirm the rather small uncertainties we could obtain this way for the two popular cosmological world models: $\Omega_m = 0.3 \pm 0.24$, $\Omega_\lambda = 0.7 \pm 0.5$ or $\Omega_m = 1.0 \pm 0.33$, $\Omega_\lambda = 0.0 \pm 1.2$. Our method can be applied from now on, on real clusters.

1 Introduction

Recent works on constraining the cosmological parameters using the CMB and the high redshift supernovae seem to converge to a new “standard cosmological model” favouring a flat universe with $\Omega_m \sim 0.3$ and $\Omega_\lambda \sim 0.7$: White⁷ and references therein. However these results are still uncertain and depend on some physical assumptions, so the flat $\Omega_m = 1$ model is still possible (Le Dour *et al.*³). It is therefore important to explore other independent techniques to constrain these cosmological parameters.

In cluster gravitational lensing, the existence of multiple images – with known redshifts – given by the same source allows to calibrate in an absolute way the total cluster mass deduced from the lens model. The great improvement in the mass modeling of cluster-lenses that includes the cluster galaxies halos (Kneib *et al.*², Natarajan & Kneib⁶) leads to the hope that clusters

can also be used to constrain the geometry of the Universe, through the ratio of angular size distances, which only depends on the redshifts of the lens and the sources, and on the cosmological parameters. The observations of cluster-lenses containing large number of multiple images lead Link & Pierce⁴ (hereafter LP98) to investigate this expectation. They considered a simple cluster potential and on-axis sources, so that images appear as Einstein rings. The ratio of such rings is then independent of the cluster potential and depends only on Ω_m and Ω_λ , assuming known redshifts for the sources. According to them, this would allow marginal discrimination between extreme cosmological cases. But real gravitational lens systems are more complex concerning not only the potential but also off-axis positions of sources. They conclude that this method is ill-suited for application to real systems.

We have re-analyzed this problem building up on the modeling technique developed by us. As demonstrated below, we reach a rather different conclusion showing that it is possible to constrain Ω_m and Ω_λ using the positions of multiple images at different redshifts and some physically motivated lens models.

Troughout this paper we have assumed $H_0 = 65 \text{ km s}^{-1} \text{ Mpc}^{-1}$, however the proposed method is independant of the value of H_0 .

2 Influence of Ω_m and Ω_λ on the images formation

2.1 Angular size distances ratio term

In the lens equation: $\theta_S = \theta_I - \frac{2}{c^2} \frac{D_{OL}D_{LS}}{D_{OS}} \nabla \phi_\theta(\theta_I)$, the dependence on Ω_m and Ω_λ is solely contained in the term $F = D_{OL}D_{LS}/D_{OS}$. For a given lens plane, $F(z_s)$ increases rapidly up to a certain redshift and then stalls, with significant differences for various values of the cosmological parameters (see Fig. 1). Thus in order to constrain the actual shape of $F(z_s)$ several families of multiple images are needed, ideally with their redshifts regularly distributed in $F(z_s)$ to maximize the range in the F variation.

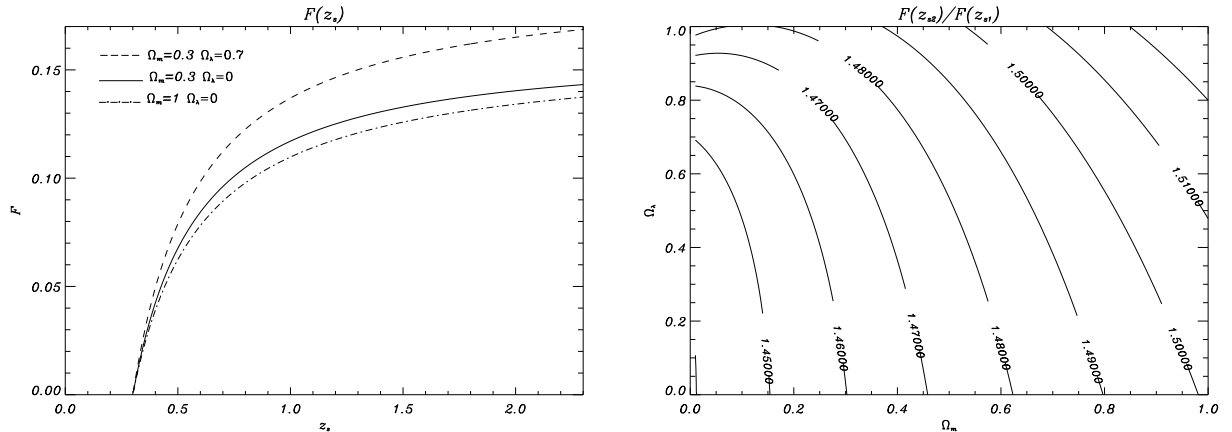


Figure 1: Left. $F(z_s)$ for $z_l = 0.3$ and various cosmological models. Right. $F(z_{s2})/F(z_{s1})$ as a function of Ω_m and Ω_λ for $z_l = 0.3$, $z_{s1} = 0.7$ and $z_{s2} = 2$.

If we consider fixed redshifts for both the lens and the sources, at least 2 multiple images are needed to derive cosmological constraints. In that case F has only an influence on the modulus of $\theta_I - \theta_S$. So taking the ratio of two different F terms provides the intrinsic dependence on cosmological scenarios, independently of H_0 . A typical configuration leads to the Fig. 1 plot. The discrepancy between the different cosmological parameters is not very large, less than 3% between an EdS model and a flat low matter density one. The figure also illustrates the

expected degeneracy of the method, also confirmed by weak lensing analyzes, with a continuous distribution of background sources (*e.g.* Lombardi & Bertin⁵).

2.2 Relative influence of the different parameters

We now look at the relative influence of the different parameters, including the lens parameters, to derive expected error bars on Ω_m and Ω_λ . To model the potential we choose the mass density distribution proposed by Hjorth & Kneib¹, characterized by a core radius, a , and a cut-off radius $s \gg a$. We can then get the expression of the deviation angle modulus $D_{\theta_I} = \|\theta_I - \theta_S\|$.

For 2 families of multiple images, the relevant quantity becomes the ratio of 2 deviation angles for 2 images θ_{I1} and θ_{I2} belonging to 2 different families at redshifts z_{s1} and z_{s2} . Let's define $R_{\theta_{I1}, \theta_{I2}} = \frac{D_{\theta_{I1}}}{D_{\theta_{I2}}}$. With several families, the problem is highly constrained because a single

potential must reproduce the whole set of images. In practice we calculate $\frac{dR_{\theta_{I1}, \theta_{I2}}}{R_{\theta_{I1}, \theta_{I2}}}$ versus the different parameters it depends on. We chose a typical configuration to get a numerical evaluation of the errors on the cosmological parameters: $z_l = 0.3$, $z_{s1} = 0.7$, $z_{s2} = 2$, $\frac{\theta_{I2}}{\theta_{I1}} = 2$, $\frac{\theta_s}{\theta_a} = 10$ ($\theta_a = a/D_{OL}$, $\theta_s = s/D_{OL}$) and we assume $\Omega_m = 0.3$ and $\Omega_\lambda = 0.7$. We then obtain the following orders of magnitudes for the different contributions :

$$\frac{dR_{\theta_{I1}, \theta_{I2}}}{R_{\theta_{I1}, \theta_{I2}}} = 0.57 \frac{dz_l}{z_l} + 0.74 \frac{dz_{s1}}{z_{s1}} + 0.17 \frac{dz_{s2}}{z_{s2}} + 0.4 \left(\frac{d\theta_{I1}}{\theta_{I1}} - \frac{d\theta_{I2}}{\theta_{I2}} \right) - 0.1 \frac{d\theta_a}{\theta_a} - 0.06 \frac{d\theta_s}{\theta_s} - 0.015 \frac{d\Omega_m}{\Omega_m} + 0.02 \frac{d\Omega_\lambda}{\Omega_\lambda} \quad (1)$$

As expected, even with 2 families of multiple images the influence of the cosmological parameters is of the second order. The precise value of the redshifts is quite fundamental, therefore a spectroscopic determination ($dz = 0.001$) is essential. The position of the (flux-weighted) centers of the images are also important. With HST observations we assume $d\theta_I = 0.1''$.

So even if the problem is less dependent on the core and cut-off radii (in other word the mass profile), they will represent the main sources of error. Taking $d\theta_a/\theta_a = d\theta_s/\theta_s = 20\%$, we then derive the errors $d\Omega_m$ and $d\Omega_\lambda$ from the above relation in the flat low matter density we chose. We did this computation for different sets of cosmological models. Indeed the errors we will obtain with this method change significantly with respect to Ω_m and Ω_λ . All other things being equal apart from the cosmological parameters, we plot $d\Omega_m$ and $d\Omega_\lambda$ for a continuous set of universe models (Fig. 2). For instance in the 2 popular cosmological scenarios, we have :

$$\Omega_m = 0.3 \pm 0.24 \quad \Omega_\lambda = 0.7 \pm 0.5 \quad \text{or} \quad \Omega_m = 1 \pm 0.33 \quad \Omega_\lambda = 0 \pm 1.2$$

As this can be easily understood from the Fig. 1 degeneracy plot, the method is in general far more sensitive to the matter density than to the cosmological constant, for which the error bars are larger.

However the results we could obtain this way are as precise as the ones given by other constraints. But these errors are just typical; provided spectroscopic and HST observations, they depend mostly on the particular cluster and the potential model chosen to describe it. They could be quite tightened with a precise model, and by increasing the number of clusters with multiple images.

3 Constraint on $(\Omega_m, \Omega_\lambda)$ from strong lensing

3.1 Method and algorithm for numerical simulations

We consider basically the potential introduced in section 2.2. After considering the lens equation, fixing arbitrary values $(\Omega_m^0, \Omega_\lambda^0)$ and a cluster lens redshift z_l , our code can determine the images

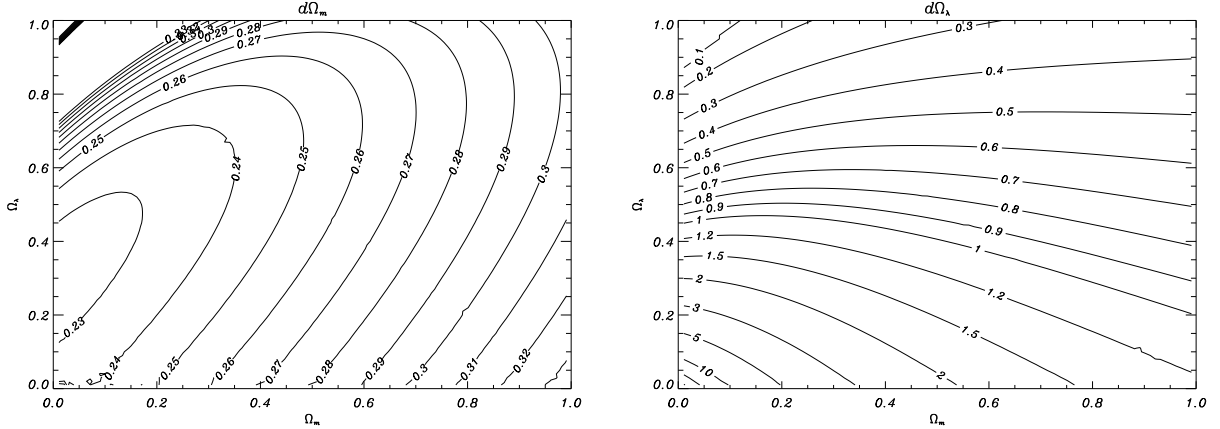


Figure 2: Expected error bars $d\Omega_m$ (Left) and $d\Omega_\lambda$ (Right) depending on the cosmological scenario with this method and in a typical case (see text).

of a source galaxy at a redshift z_s . Then taking as single observables these sets of images as well as the different redshifts, we can recover some parameters (the more important ones being σ_0 , θ_a or θ_s) of the potential we left free for each point of a grid $(\Omega_m, \Omega_\lambda)$. The likelihood of the result is obtained via a χ^2 -minimization, where the χ^2 is computed in the source plane as follows :

$$\chi^2 = \sum_{i=1}^n \sum_{j=1}^{n^i} \frac{(\theta_{Sj}^i - \theta_{SG}^i)^2}{\sigma_{Si}^{j2}} \quad (2)$$

The subscript i refers to the families and the subscript j to the images of a family. There is a total of $\sum_{i=1}^n n^i = N$ images. θ_{Sj}^i is the source found for the image θ_{Ij}^i in the inversion. θ_{SG}^i is the barycenter of the θ_{Sj}^i (belonging to a same family). Finally if θ_{Ii}^j is the error on the position of the center of θ_{Ij}^i and A_j^i the amplification for this image, then $\sigma_{Si}^j = \sigma_{Ii}^j / \sqrt{A_j^i}$.

3.2 Numerical simulations in a typical configuration

To recover the parameters of the potential (*i.e.* σ_0 , θ_a , θ_s and adjusted lens parameters), we generated 3 families of images with regularly distributed source redshifts.

For starting values $(\Omega_m^0, \Omega_\lambda^0) = (0.3, 0.7)$ we obtained confidence levels shown in Fig. 3. The method puts forward a good constraint, better on Ω_m than on Ω_λ , and the degeneracy is the expected one (see Fig. 1). Concerning the free parameters, we also recovered in a rather good way the potential, the variations being $\Delta\sigma_0 \sim 150$ km/s, $\Delta\theta_a \sim 3''$ and $\Delta\theta_s \sim 20''$.

This is an “ideal” case, of course, because we tried to recover the same type of potential we used to generate the images, the morphology of the cluster being quite regular and the redshift range of the sources being wide enough to check each part of the F curve. Such a simple approach can be applied to regular clusters like MS2137-23, which shows at least 3 families of multiple images including a radial one, see Fig. 4. But the spectroscopic redshifts are still currently missing for this cluster.

4 Conclusions & prospects

Following the work of LP98, we discussed a method to obtain informations on the cosmological parameters Ω_m and Ω_λ while reconstructing the lens gravitational potential of clusters with multiple image systems at different redshifts.

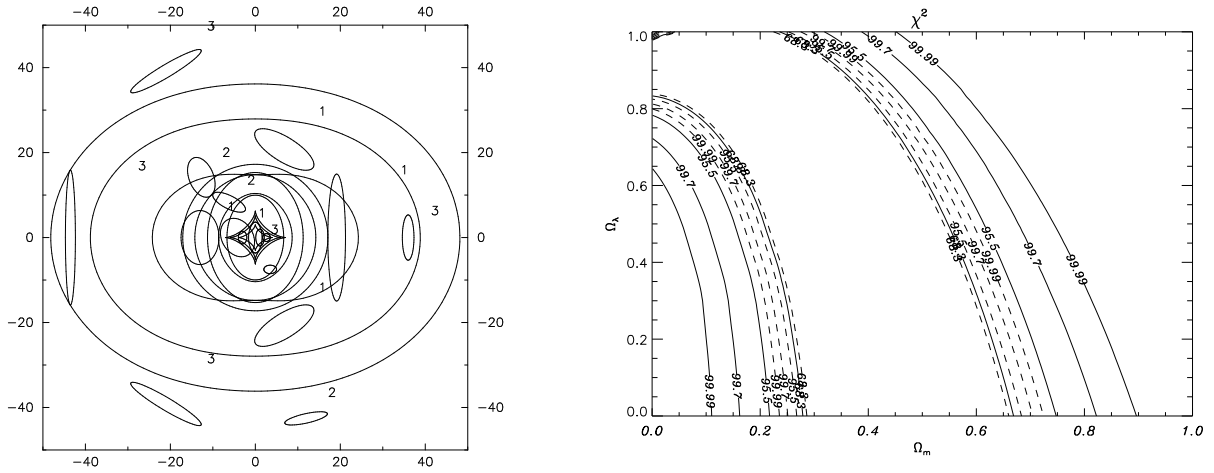


Figure 3: Left. Generation of images by a $z_l = 0.3$ cluster with $\sigma_0 = 1400$ km/s, $\theta_a = 13.54''$ and $\theta_s = 145.8''$. Close to their respective critic lines, we see 3 families of images at $z_{s1} = 0.6$, $z_{s2} = 1$ and $z_{s3} = 2$. Right. Solid lines : $\chi^2(\Omega_m, \Omega_\lambda)$ confidence levels obtained for this configuration. Generating arbitrary values: $(\Omega_m^0, \Omega_\lambda^0) = (0.3, 0.7)$. Dashed lines: $\chi^2(\Omega_m, \Omega_\lambda)$ confidence levels obtained considering 10 clusters in this same configuration.

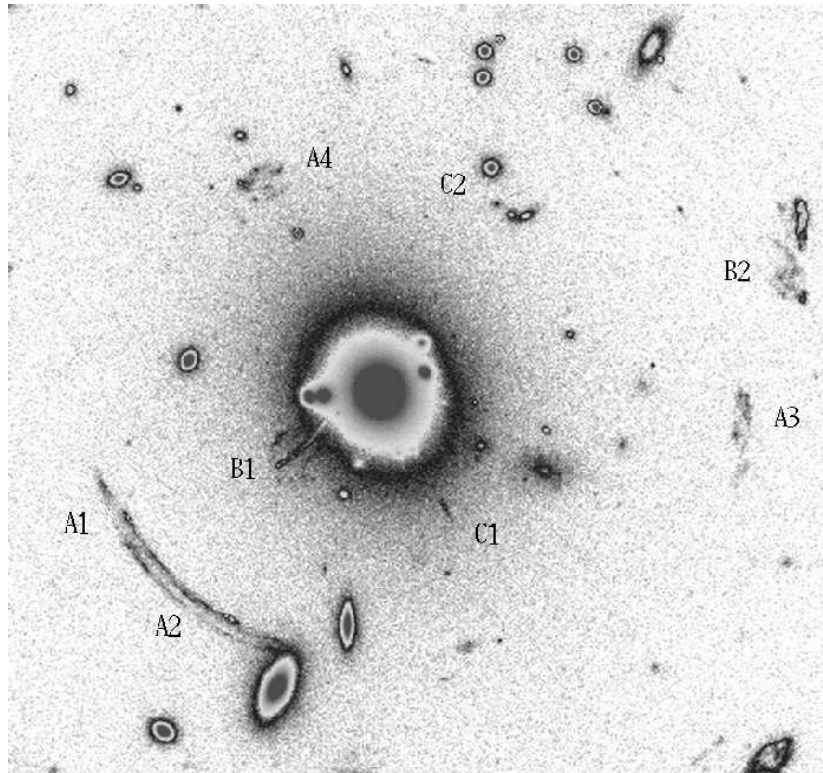


Figure 4: HST image of MS2137-23 ($z_l = 0.313$). We see 3 families of images, a tangential arc A1-A2 with its associated arcs A3 and A4, and 2 radial arcs B1 and C1 with their associated images B2 and C2.

This technique gives degenerate constraints, Ω_m and Ω_λ being negatively correlated, with a better constraint of the matter density. With a single cluster in a typical lensing configuration we can expect the following error bars : $\Omega_m = 0.3 \pm 0.24$, $\Omega_\lambda = 0.7 \pm 0.5$. To perform that, several general conditions must be fulfilled:

- * a cluster with a rather regular morphology, so that a few parameters are needed to describe the gravitational potential ; this is not so restrictive because we saw that a bimodal cluster can also provide a constraint,

- * “numerous” systems of multiple images, probing each part of the cluster,

- * a good spatial resolution image (HST observations) of the cluster and arcs to compute relatively precise – 0.1” – (flux weighted) images positions,

- * spectroscopic precision for the different redshifts that should be also regularly distributed from z_l to high values – this requires deep spectroscopy on 8-10m class telescopes due to the faintness of the multiple images .

It is important to notice that one cluster could provide one constraint on the geometry of the whole universe. And it is possible to combine data from different clusters to tighten the error bars. Combining the study of about 10 clusters would lead to meaningful constraints. The dashed lines confidence levels in the Fig. 3 are the result of a numerical simulation made with 10 *identical* clusters.

Actually the degeneracy depends only on the different redshifts involved that we will have various sets of when applying the method to real configurations. This should lead to a more reduced area of allowed cosmological parameters. We are encouraged by more and more known observations including systems with multiple sources and we plan to apply this technique to clusters like MS2137-23, MS0440+02, A370, AC114 and A1689.

References

1. J. Hjorth and J.-P. Kneib, submitted to *ApJ* (1999).
2. J.-P. Kneib, R. Ellis, I. Smail, W. Couch & R. Sharples, *ApJ* **471**, 643 (1996).
3. M. Le Dour, M. Douspis, J. Bartlett & A. Blanchard, astro-ph/0004282, submitted to *A&A* (2000).
4. R. Link and M. Pierce, *ApJ* **502**, 63 (1998).
5. M. Lombardi and G. Bertin, *A&A* **342**, 337 (1998).
6. P. Nararajan & J.-P. Kneib, *MNRAS* **287**, 833 (1997).
7. M. White, *ApJ* **506**, 495 (1998).